Estimation of the acoustic wavefield generated by a seismic vessel from towed streamer data

Stian Hegna, PGS*

Summary

Imaging the subsurface using passive data acquired with a towed streamer configuration is discussed in this paper. Instead of an active source, the acoustic wavefield generated by the seismic vessel is used for imaging the subsurface. The primary purpose of this work was to test the feasibility of estimating the wavefield emitted from the seismic vessel using data recorded by towed streamers and using this wavefield for imaging the subsurface. After a description of a method for estimating the acoustic wavefield generated by the seismic vessel from towed streamer data acquired without an active source, a data example from offshore Malaysia will be shown. The acoustic signals generated by the seismic vessel have been estimated from recorded hydrophone data. This estimation is limited to frequencies above 30 Hz since non-acoustic noise dominates over the weak acoustic signals generated by the vessel at lower frequencies. Results from imaging the passive data using the estimated acoustic signals from the seismic vessel are compared with imaging the subsurface based on seismic data acquired with airguns.

Introduction

Even though seismic vessels are designed to generate as little noise and vibrations in the hull as possible, some acoustic signals are generated. These signals respond to the local geology and are received by the sensors in the streamers towed behind the vessel. This acoustic wavefield originating from the seismic vessel itself is generally not treated as a signal in the imaging of marine seismic data and is typically categorized as ambient noise. However, if these acoustic signals could be characterized, this ambient noise that is also referred to as ship noise could be attenuated. Alternatively, the ship noise may be used to image the subsurface, possibly as a complement to images based on seismic data acquired with active source(s).

Using recorded ambient noise for imaging the subsurface is well known. Seismic interferometry techniques, based on cross-correlating traces recorded in different positions, are used to retrieve information about the subsurface without knowledge of the source wavefield. Different seismic interferometry approaches are discussed in Wapenaar *et al.* (2004). Another possible method is up/down deconvolution described by Amundsen (2001). This is a method for eliminating the effect of the free surface from marine seismic data. The source wavefield is deconvolved as part of the process. A third possible method is imaging with separated wavefields, discussed in Whitmore *et al.* (2010). In common with up-down deconvolution, this method requires separated up- and down- going wavefields as input. To image the primary reflections without knowledge of the source wavefield, the direct wavefield needs to be recorded and included in the down-going wavefield after wavefield separation.

There are, however, challenges to applying these methods to passive data acquired with towed streamers. The fact that acoustic signals are generated continuously by the seismic vessel in combination with a passive source and receivers that are moving all the time means that seismic data recorded continuously cannot be split into natural common 'shot' or receiver gathers. Another challenge is that the receivers are mounted in streamers and typically towed at relatively shallow depths and a long distance behind the seismic vessel. A typical towing setup with a large streamer spread is shown in Figure 1.

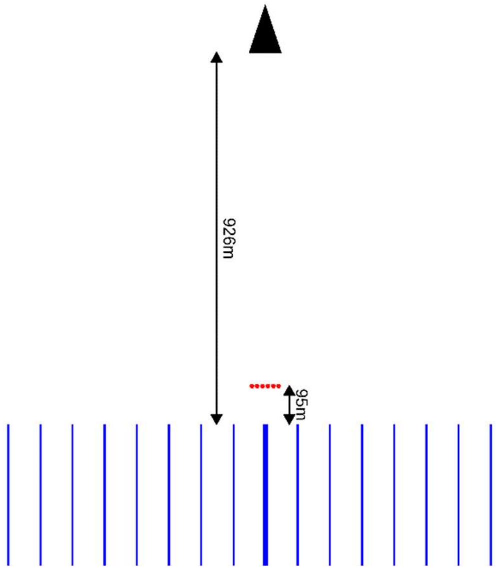

Figure 1: Inline distance between the seismic vessel (black triangle) and the streamer fronts (blue lines), and between airgun arrays (red dots) and streamer fronts.

This means that the near-vertical part of the source wavefield that goes into the ground is not recorded. Therefore, an approach that is more similar to what is normally used for seismic data acquired with active source(s) has been used in this work, where the wavefield emitted by the passive source is estimated and deconvolved from the received wavefield. Estimation of the acoustic wavefield generated by the seismic vessel from data acquired without an active source will be discussed in this paper. In addition, the continuous wavefields method, first introduced in Hegna *et al.* (2018), is used to retrieve information about the subsurface. This method is designed to handle continuous wavefields on both the source and the receiver side in combination with moving sources and receivers. Hence, it is well suited to seismic data acquired without an active source, provided that the wavefield emitted from the passive source is known.

Method

In the case of towed streamer acquisition, the direct wave recorded by the streamers is a measurement that can be used to estimate the acoustic signals generated by the seismic vessel emitted in the direction towards the streamers. This wavefield is likely to be directional. Consequently, the near-vertical part of the wavefield that goes into the ground is most likely not identical to the part of the wavefield emitted in the direction towards the streamers. Therefore, when estimating the wavefield generated by the vessel using the direct wave recorded by the streamers, there are most likely some errors in the results after deconvolving the source wavefield from the received wavefield.

The wavefield recorded by the streamers contains both the direct wave as well as the wavefield that has propagated through water and into to the subsurface. Therefore, before estimating the wavefield generated by the seismic vessel, the signals coming from the direction of the seismic vessel, i.e. close to 90 degrees emergent angle, are isolated. The direct wave itself can be described as a convolution of the signals emitted from the source in the direction towards the streamers with an operator describing the propagation of the wavefield from the location of the vessel to the location of the receivers mounted in the streamers. This propagation operator can be expressed as

$$P(\omega) = \frac{1}{N}\sum_{n=1}^{N}\left[\frac{e^{-i\omega r_n/c}}{r_n} + R\,\frac{e^{-i\omega r'_n/c}}{r'_n}\right] \qquad (1)$$

where ω is the angular frequency, N is the number of receivers in the receiver array, r_n is the distance from the source to receiver n in the receiver array, c is the velocity of sound in water, R is the reflection coefficient at the sea surface (close to -1), and r'_n is the distance from the source to receiver n in the receiver array via the sea surface.

The direct wave $D(\omega)$ can be expressed as

$$D(\omega) = S(\omega)P(\omega)R_{sens}(\omega) \qquad (2)$$

where $S(\omega)$ is the emitted source wavefield at an angular frequency ω, and $R_{sens}(\omega)$ is the response of the receiver array and its sensors at the same angular frequency. An estimate of the wavefield emitted from the source $\tilde{S}(\omega)$ can be derived using the following equation,

$$\tilde{S}(\omega) = \widetilde{D}(\omega)[P(\omega)R_{sens}(\omega)]^{-1} \qquad (3)$$

where $\widetilde{D}(\omega)$ is the seismic data measured by a receiver array after having isolated the signals coming from the direction of the source. Since there are many receiver arrays in each streamer, and several streamers towed behind the vessel, data from many receiver arrays can be used to estimate the wavefield emitted from the source (in this case ship noise). These estimates can be stacked to obtain one estimate of the source wavefield. The distances between the source and the receivers tend to vary slightly during seismic acquisition. To take these variations into account, the source wavefield may therefore be estimated in overlapping time windows, e.g. in the order of 10-20 seconds long.

Examples

More than one hour of "passive" seismic data were acquired without triggering any airguns during a field test of the continuous wavefields method acquired offshore Malaysia late 2019, that was discussed in Klüver *et al.* (2020). These passive data were acquired along the same line trajectories as used for the acquisition of continuous seismic data where individual airguns were triggered with short random time intervals. The upper row in Figure 2 shows examples of a two second time window for seismic data recorded when triggering airguns, and when recording without triggering airguns for comparison. The amplitude increase around channel 105 visible in the middle and right columns in the upper row of Figure 2 is related to signals reflected at an angle close to the critical angle. These reflected signals are most likely associated with the acoustic wavefield generated by the seismic vessel itself, since the ship noise is the main source of acoustic signals during the recording of these data.

Figure 2 also includes frequency-wavenumber spectra of the same data. The acoustic signals associated with the emitted source wavefield and the response of the earth is clearly visible within the signal cone in both the data acquired with airgun sources and the data acquired without an active source. In the data acquired without an active source, signals associated with the seismic vessel and its response from the earth, are not visible below 25-30 Hz due to high levels of non-acoustic noise relative to the weak acoustic signals generated by the seismic vessel. Therefore, it is difficult to estimate the acoustic wavefield generated by the vessel below ~30 Hz from these hydrophone data.

When estimating the acoustic wavefield generated by the seismic vessel, the signals coming from the direction of the seismic sources, i.e. close to 90 degrees emergent angle in the frequency – wavenumber spectra shown in the middle and right columns in the bottom row of Figure 2, have been isolated.

10.1190/segam2021-3580679.1

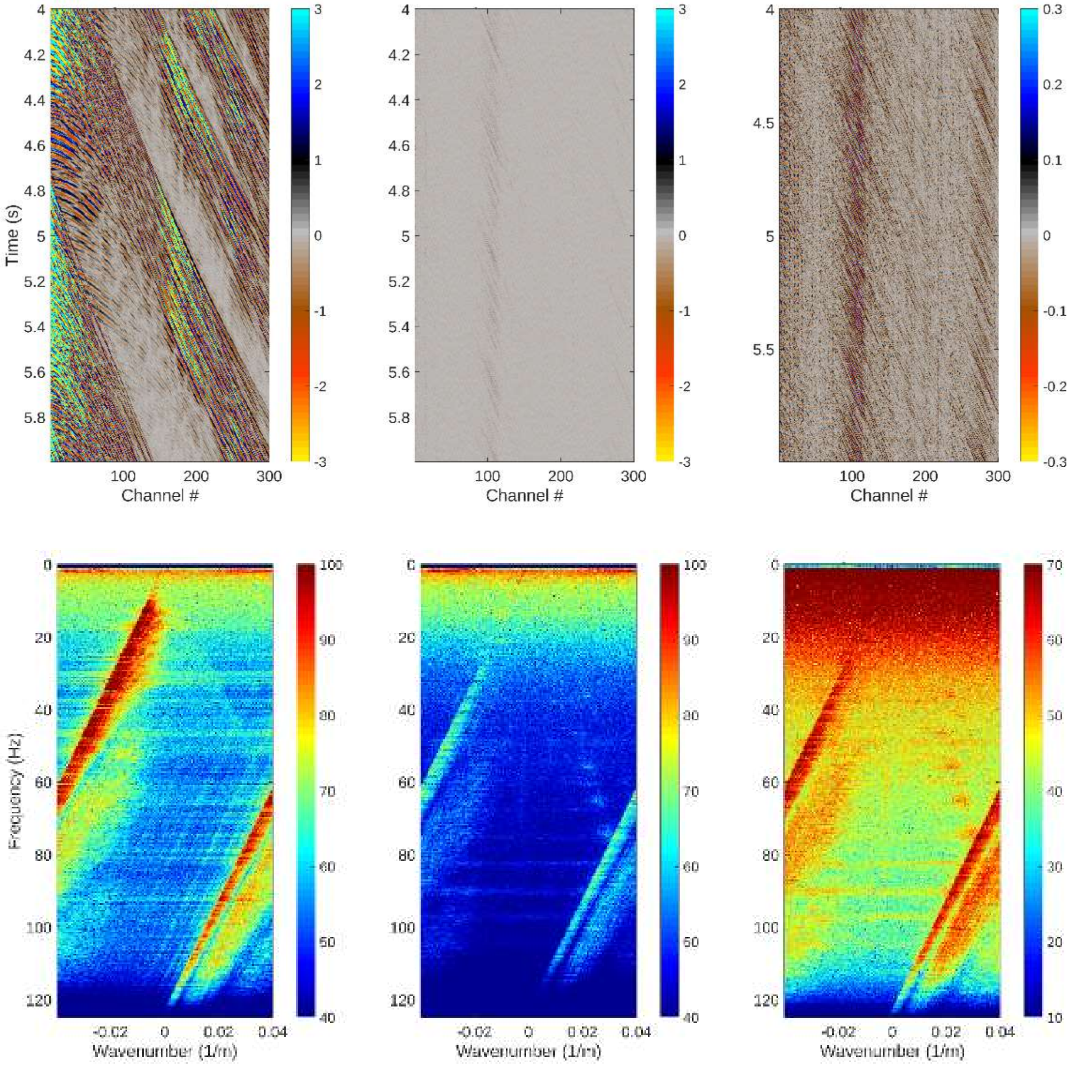

Figure 2: Examples of recorded hydrophone data when triggering airguns (left column), and when recording data without triggering any airguns (middle and right columns). In the column on the right the limits of the color scales have been adjusted so that the acoustic signals are more visible. The top row shows the data in time and along the streamer, whereas the bottom row shows frequency-wavenumber spectra of the same data where the temporal length of the data going into the Fourier transforms is more than 40 minutes.

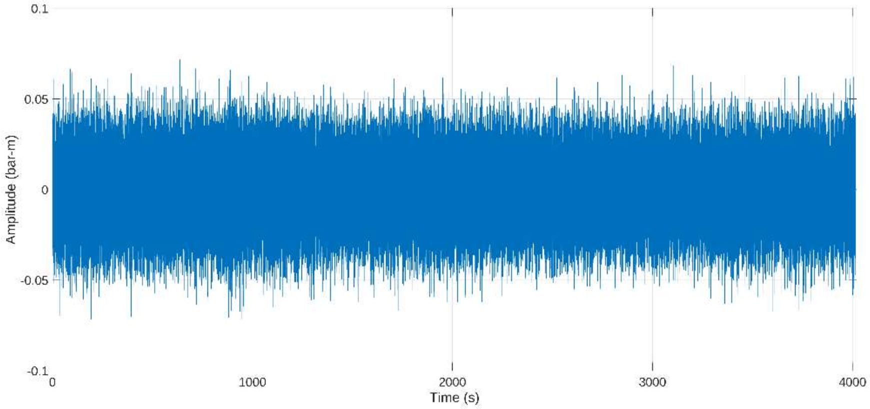

Figure 3: Estimated acoustic signals (pressure in bar at 1 m from the source) generated by the seismic vessel as a function of time, emitted in the direction towards the streamers.

The estimation has been performed using Equation 3 for time windows of 20 seconds with 10 seconds of overlap between them. Figure 3 shows the estimated acoustic signals generated by the seismic vessel.

The estimated acoustic signals generated by the seismic vessel were deconvolved from the received wavefield using the iterative multidimensional deconvolution described in Hegna *et al.* (2018). The resulting gathers were migrated and stacked to obtain a seismic image of the subsurface. The data acquired when triggering airguns with short random time intervals were processed using a similar workflow as for the data acquired without an active source for comparison. Since the vessel was ~830 m in front of the active sources as illustrated in Figure 1, an offset range similar to the offset range available in the data acquired without an active source was selected before stacking. In addition, signals below 30 Hz were filtered out since it was difficult to estimate the acoustic signals generated by the seismic vessel below this frequency. A comparison between the results is shown in Figure 4.

Conclusions

The acoustic signals generated by the seismic vessel have been estimated by isolating the signals coming from the direction of the seismic vessel, and backpropagating the resulting signals from the receiver locations to the location of the seismic vessel. The estimation of this source wavefield is limited to above 30 Hz since the recorded hydrophone data were dominated by non-acoustic noise below this frequency. The continuous wavefields method has been used to pre-process the recorded hydrophone data together with the estimated source wavefield, and then migrated and stacked to obtain an image of the subsurface. A comparable image has been produced based on data acquired by triggering individual airguns with short and random time intervals. There are clear similarities between these images; however, there are obvious differences too. These differences are likely to be related to errors in the estimated acoustic signals generated by the seismic vessel. Further work is needed to improve the estimation of the wavefield generated by the seismic vessel. Nevertheless, these results serve to demonstrate the feasibility of using streamer data to derive an unknown source wavefield with sufficient accuracy to image the subsurface.

Acknowledgements

Many thanks to PGS for supporting this work.

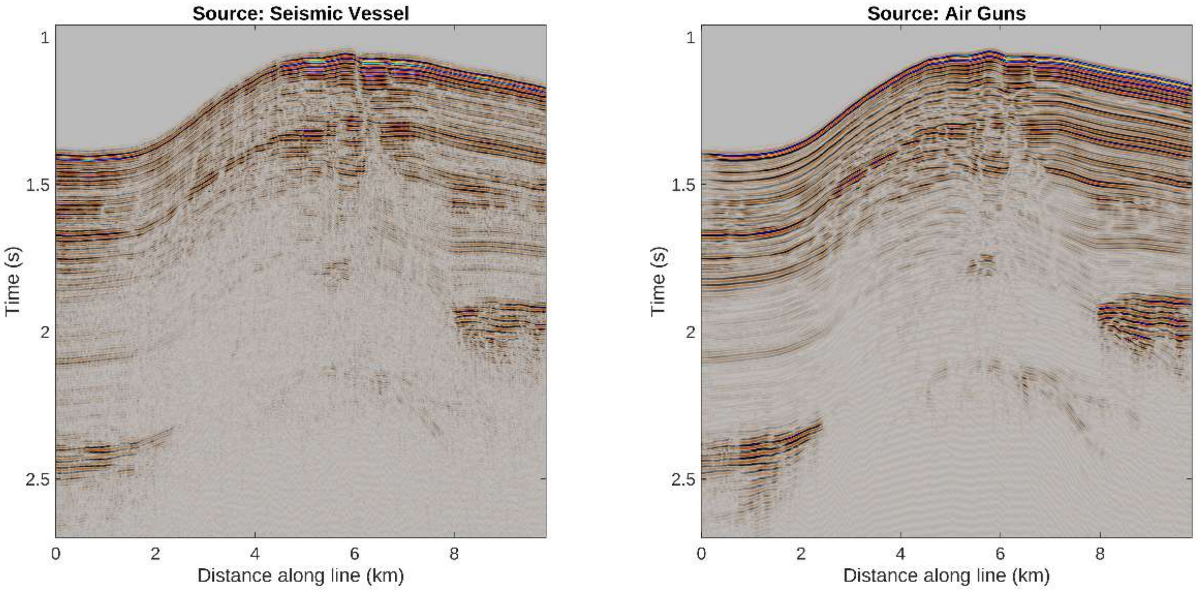

Figure 4: Comparison between a seismic image derived from data recorded without an active source using the acoustic signals generated by the seismic vessel as the source (left), and an image produced from data acquired by triggering individual airguns with short random time intervals (right).

References

Amundsen, L., 2001, Elimination of free-surface related multiples without need of the source wavelet: Geophysics, **66**, 327–341, doi: https://doi.org/10.1190/1.1444912.

Hegna, S., T. Klüver, and J. Lima, 2018, Making the transition from discrete shot records to continuous wavefields – Methodology: 80th Annual International Conference and Exhibition, EAGE, Extended Abstracts, We LHR2 06, doi: https://doi.org/10.3997/2214-4609.201800999.

Klüver, T., S. Hegna, and Lima, J., 2020, Continuous wavefields method – Insights from a shallow water field trial: 90th Annual International Meeting, SEG, Expanded Abstracts, 1–5, doi: https://doi.org/10.1190/segam2020-3426955.1.

Wapenaar, K., D. Draganov, J. van der Neut, and J. Thorbecke, 2004, Seismic interferometry: a comparison of approaches: 74th Annual International Meeting, SEG, Expanded Abstracts, 1981–1984, doi: https://doi.org/10.1190/1.1851182.

Whitmore, N. D., A. A. Valenciano, W. Sollner, and S. Lu, 2010, Imaging of primaries and multiples using a dual- sensor towed streamer: 80th Annual International Meeting, SEG, Expanded Abstracts, 3187–3192, doi: https://doi.org/10.1190/1.3513508.